*Article*

# Integration of mRNA and miRNA Analysis Reveals the Molecular Mechanism Underlying Salt and Alkali Stress Tolerance in Tobacco

**Jiayang Xu [1], Qiansi Chen [2], Pingping Liu [2], Wei Jia [3], Zheng Chen [1] and Zicheng Xu [1,*]**

[1] National Tobacco Cultivation and Physiology and Biochemistry Research Center, College of Tobacco Science, Henan Agricultural University, Zhengzhou 450002, China; jiayangxu@126.com (J.X.); zchen1004@126.com (Z.C.)

[2] Zhengzhou Tobacco Research Institute, Zhengzhou 450001, China; chen_qiansi@163.com (Q.C.); Liu_pingping2012@163.com (P.L.)

[3] College of Resources and Environment, Huazhong Agricultural University, Wuhan 430070, China; shuhan_jia@163.com

* Correspondence: zichengxu@126.com; Tel.: +86-371-63555916

check for updates

**Abstract:** Salinity is one of the most severe forms of abiotic stress and affects crop yields worldwide. Plants respond to salinity stress via a sophisticated mechanism at the physiological, transcriptional and metabolic levels. However, the molecular regulatory networks involved in salt and alkali tolerance have not yet been elucidated. We developed an RNA-seq technique to perform mRNA and small RNA (sRNA) sequencing of plants under salt (NaCl) and alkali (NaHCO$_3$) stress in tobacco. Overall, 8064 differentially expressed genes (DEGs) and 33 differentially expressed microRNAs (DE miRNAs) were identified in response to salt and alkali stress. A total of 1578 overlapping DEGs, which exhibit the same expression patterns and are involved in ion channel, aquaporin (AQP) and antioxidant activities, were identified. Furthermore, genes involved in several biological processes, such as "photosynthesis" and "starch and sucrose metabolism," were specifically enriched under NaHCO$_3$ treatment. We also identified 15 and 22 miRNAs that were differentially expressed in response to NaCl and NaHCO$_3$, respectively. Analysis of inverse correlations between miRNAs and target mRNAs revealed 26 mRNA-miRNA interactions under NaCl treatment and 139 mRNA-miRNA interactions under NaHCO$_3$ treatment. This study provides new insights into the molecular mechanisms underlying the response of tobacco to salinity stress.

**Keywords:** salt; alkali; transcriptome; miRNA; tobacco

## 1. Introduction

Salinity stress is one of the most constraining environmental factors that threatens both the productivity and quality of crop plants worldwide [1]. In China, a large amount of land is unsuitable for agricultural production because of increasing soil alkalinity. Terrestrial soils affected by salt are divided mainly into saline soils, alkaline soils and salt-alkaline soils [2]. NaCl is a major neutral component that causes salt stress, and NaHCO$_3$ and Na$_2$CO$_3$ play a key role in soil alkalization with increasing pH. By causing osmotic stress, ion toxicity, redox imbalance and metabolic damage, soil salinity and salinization can severely affect biological homeostasis in plants [3,4]. Plants have evolved strategies to cope with salt stress. These strategies include increased accumulation of compatible solutes such as proline, soluble sugars and betaine to adjust to osmotic injury [5]; activation of reactive oxygen species (ROS) scavenging systems to protect plants against oxidative damage triggered by salinity [6]; and regulation of the expression of salt-responsive genes to re-establish ion homeostasis

and protect cellular machinery from stress [7,8]. Therefore, to reduce the decrease in crop yield and quality caused by salt stress and promote crop improvement, it would be of great value to understand the molecular mechanism underlying salt tolerance in crop plants.

MicroRNAs (miRNAs) are endogenous, short (18–24 nt), non-coding RNA molecules that negatively regulate gene expression at the post-transcriptional and translational levels [9,10]. A total of 8496 mature miRNAs from 73 plant species have been identified [11]. Many experimental studies have demonstrated that miRNAs play crucial roles in processes associated with plant growth and development, such as cell differentiation [12], organ development [13,14] and flowering [15,16]. In addition to these roles in physiological and metabolic processes, many studies have also shown that miRNAs are widely involved in plant responses to abiotic stress, including drought [17], heat [18], cold [19] and salt stress [20].

Next-generation sequencing (NGS) technology provides a comprehensive understanding of gene status and has become an accurate molecular analytical tool for transcriptional profiling experiments [21]. This sequencing approach has been successfully used to identify the expression of salt-responsive genes in cotton [22], wheat [23], soybean [24], rice [25] and citrus [26]. Moreover, revealing the miRNA-mediated regulatory network of the salt stress response will provide a genetic basis for future studies. A large number of studies have identified many salt stress-related miRNAs in various plant species, such as Arabidopsis [27], wheat [28], cucumber [29], barley [30] and maize [31].

Tobacco (*Nicotiana tabacum* L.) is an important commercial species that is widely cultivated worldwide. Moreover, this plant species is recognized as an excellent model system in plant science for studies on physiological and molecular mechanisms [32,33]. The draft genome sequences of two tobacco species (*N. tabacum* and *Nicotiana benthamiana*) provide a global functional description of identified genes for crop improvement and basic research [34,35]. Although some salt stress-related genes and miRNA profiles have been characterized in tobacco [36,37], our focus here is an integrated analysis of mRNA and miRNA profiling in tobacco under different types of salt and alkali stress.

## 2. Results

### 2.1. mRNA Sequencing Data Analysis

A total of nine qualified libraries from the control (CK), NaCl (salt stress, SS) and NaHCO$_3$ (alkali stress, AS) treatments, with three replicates per treatment, were sequenced. An overview of the sequencing and assembly data is provided in Table 1. After removal of the low-quality reads from the raw data, approximately 22.14, 26.21 and 26.70 Gb of clean reads were obtained in the CK, SS and AS groups. More than 93.2% of the reads had Q-scores at the Q30 level (an error threshold of less than 0.01%), and more than 93.5% of the clean reads were aligned. To evaluate the gene expression reliability among these replicates, Pearson correlation analysis was conducted. As shown in Figure 1, the results of the correlation analysis indicated that tobacco exhibited more than 85% similarity among the CK, SS and AS treatments.

**Table 1.** Summary of mRNA sequencing datasets.

| Treatment | Raw Reads | Clean Reads | Clean Bases | Q30 (%) | Mapped Reads |
|---|---|---|---|---|---|
| CK_1 | 55,946,150 | 54,753,170 | 8.21 G | 93.32 | 51,560,453 (94.17%) |
| CK_2 | 52,426,666 | 50,127,414 | 7.52 G | 93.82 | 47,158,934 (94.08%) |
| CK_3 | 43,620,248 | 42,722,964 | 6.41 G | 93.71 | 40,181,708 (94.05%) |
| SS_1 | 51,641,948 | 50,378,090 | 7.56 G | 93.54 | 47,605,747 (94.5%) |
| SS_2 | 61,792,742 | 60,177,334 | 9.03 G | 93.74 | 56,855,737 (94.48%) |
| SS_3 | 65,172,280 | 64,106,196 | 9.62 G | 93.64 | 60,509,819 (94.39%) |
| AS_1 | 64,693,340 | 63,648,474 | 9.55 G | 93.49 | 59,519,456 (93.51%) |
| AS_2 | 58,326,842 | 57,264,752 | 8.59 G | 93.49 | 53,875,061 (94.08%) |
| AS_3 | 57,919,408 | 57,037,200 | 8.56 G | 93.24 | 53,759,723 (94.25%) |
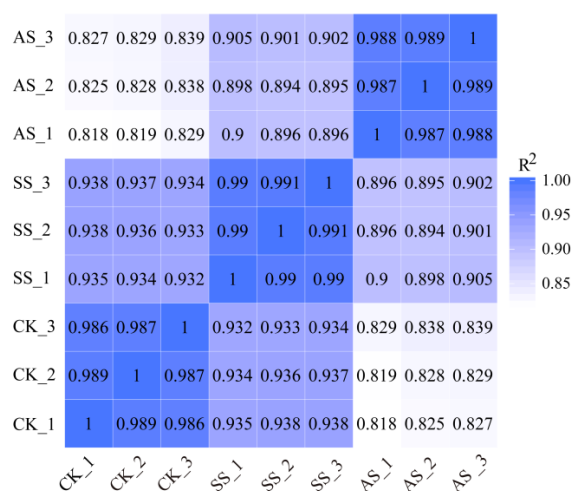


**Figure 1.** Heatmap of Pearson correlations of the expression levels among samples. CK: control samples, SS: 100 mM NaCl-treated samples, AS: 100 mM NaHCO$_3$-treated samples. The numbers in the boxes refer to Pearson's correlation coefficients ($R^2$ values). The number "1" in the boxes represents a high degree of correlation.

## 2.2. Differentially Expressed Genes under Salt-Alkali Stress

To identify genes that are differentially regulated under various salt-alkali conditions, we used the DESeq software to perform a differential expression analysis between the treatment and CK samples. With strict criteria of $|\log_2 FC| > 2$ and *p*-value less than 0.05 ($|\log_2 FC| > 2$, $p < 0.05$), a total of 2206 genes (Table S1) and 7468 genes (Table S2) were found to be differentially expressed in response to SS and AS, respectively (Figure 2A). There were many more differentially expressed genes (DEGs) in the AS treatment than in the SS treatment, indicating that NaHCO$_3$ treatment induced a significantly greater number of biological and metabolic changes than did the NaCl treatment. To better characterize the salt-alkali stress-induced changes in gene expression in tobacco, the overlapping DEGs between the SS vs. CK and AS vs. CK comparable groups are shown as a Venn diagram in Figure 2B. Detailed analysis of these 1610 overlapping DEGs revealed that 1578 of them exhibited the same trends under salt-alkali stress: 828 genes were upregulated and 750 genes were downregulated in both the SS vs. CK and AS vs. CK comparisons.
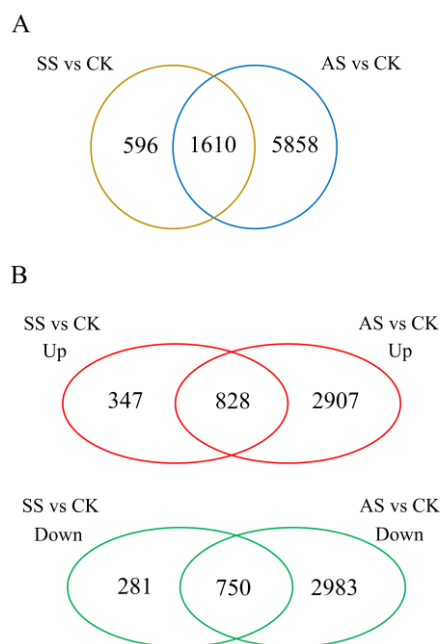
**Figure 2.** Differential gene expression analysis of the SS vs. CK and AS vs. CK comparisons. (**A**) Venn diagram of overlapping differentially expressed genes (DEGs) among salt-alkali stress comparisons. (**B**) Venn diagrams illustrating the overlap between the upregulated and downregulated genes in the SS vs. CK and AS vs. CK comparisons.

*2.3. Functional Classification of Salt-Alkali Responsive Genes*

To better understand the functions of the DEGs, we mapped all of these salt-alkali responsive genes to the Gene Ontology (GO) database. In total, we identified 92 and 206 significantly enriched GO terms (false discovery rate (FDR) < 0.05) in the SS and AS treatments, respectively (Table S3). Among these GO terms, some crucial biological processes related to "response to water (GO: 0009415)," "antioxidant activity (GO: 0016209)" and "oxidoreductase activity (GO: 0016491)" were observed in both the SS and AS treatments, while genes involved in "photosystem (GO: 0009521)," "cellular carbohydrate metabolic process (GO: 0044262)," "glucan metabolic process (GO: 0006073)" and "defense response (GO: 0006952)" were enriched in only the AS treatment.

Kyoto Encyclopedia of Genes and Genomes (KEGG) pathway analysis provided information concerning gene function. A total of 13 and 24 pathways were enriched in the SS and AS treatments, respectively (Figure 3). The enriched KEGG pathways revealed that the DEGs detected under salt-alkali stress were enriched in "photosynthesis-antenna proteins," "plant hormone signal transduction" and "glucosinolate biosynthesis". Fourteen KEGG pathways, including "photosynthesis," "starch and sucrose metabolism," "glutathione metabolism" and "carbon fixation in photosynthetic organisms," were specifically enriched in the AS treatment. These results suggest that the DEGs identified in this study may play important roles in salt and alkali stress in tobacco.
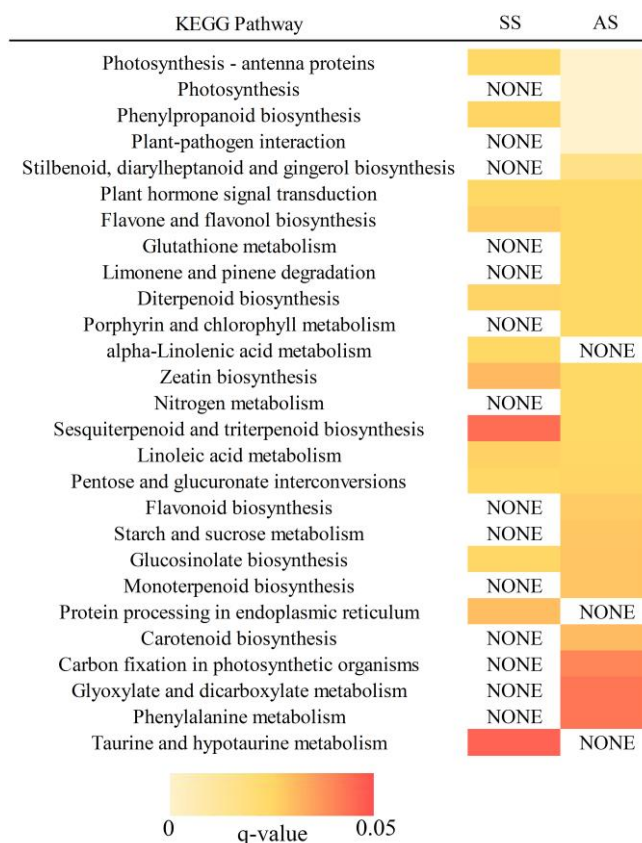
**Figure 3.** Heatmap of Kyoto Encyclopedia of Genes and Genomes (KEGG) pathway analysis of DEGs in the SS and AS treatments. A total of 13 and 24 enriched KEGG pathways were identified in the SS and AS samples, respectively. The box colour represents the q-value of the pathway.

*2.4. miRNA Sequencing Data Analysis*

Nine small RNA (sRNA) libraries were constructed with three biological replicates for the CK, SS and AS treatments. A total of 44,642,448, 39,911,768 and 42,157,754 raw reads were obtained from the CK, SS and AS samples, respectively. After the adapter sequences, poly-A sequences, low-quality reads and reads shorter than 18 nt were discarded, 43,327,623, 38,719,988, and 40,868,990 clean reads were obtained from the CK, SS and AS samples, respectively. A majority of the sRNAs were 21–24 nt in length in all nine libraries, with 24 nt being the most frequent length (Figure S1). On the basis of the method described above, a total of 88 mature miRNAs and 102 novel miRNAs were identified in these nine sRNA libraries (Table S4). Details concerning the distribution of the sRNAs are provided in Table 2.

**Table 2.** Summary of small RNA (sRNA) sequencing datasets.

| Treatment | Raw Reads | Clean Reads | Mature miRNAs | Novel miRNAs |
|-----------|-----------|-------------|---------------|--------------|
| CK_1 | 15,192,456 | 14,706,127 | 79 | 99 |
| CK_2 | 16,160,064 | 15,672,009 | 74 | 99 |
| CK_3 | 13,289,928 | 12,949,487 | 67 | 99 |
| SS_1 | 13,583,796 | 13,079,201 | 80 | 100 |
| SS_2 | 12,296,168 | 11,973,197 | 72 | 97 |
| SS_3 | 14,031,804 | 13,667,590 | 76 | 100 |
| AS_1 | 13,551,741 | 13,090,227 | 80 | 99 |
| AS_2 | 15,333,030 | 14,915,331 | 78 | 98 |
| AS_3 | 13,272,983 | 12,863,432 | 81 | 101 |

### 2.5. Differential Expression of miRNAs in Response to Salt-Alkali Stress

With respect to the miRNA-seq data analysis, a total of 33 differentially expressed miRNAs (DE miRNAs) were detected in the SS and AS treatments with the criteria |log$_2$FC|> 0.5 and *p*-value < 0.05, 16 of which were identified as novel miRNAs (Table 3). Five conserved and 10 novel miRNAs were significantly differentially expressed under SS conditions, four of whose expression was upregulated and 11 of whose was downregulated. Fourteen conserved and eight novel miRNAs were differentially expressed in response to AS, and among those miRNAs, compared with that of the CK, the expression of 13 and nine was upregulated and downregulated, respectively. Of these 33 DE miRNAs, four, namely, nta-miR156a, nta-miR6149a, miR-novel_64 and miR-novel_216, that overlapped between the SS and AS samples were identified. As expected, with the exception of nta-miR156a, all of these overlapping DE miRNAs exhibited similar regulation of expression under the SS and AS treatments.

**Table 3.** List of differentially expressed microRNAs (DE miRNAs) in response to SS and AS treatments.

| miRNA | log$_2$FC | *p*-Value | Mature Sequence | Regulated |
|---|---|---|---|---|
| nta-miR156a | −0.64 | $2.56 \times 10^{-2}$ | UGACAGAAGAGAGUGAGCAC | SS |
| nta-miR396a | 0.64 | $1.07 \times 10^{-3}$ | UUCCACAGCUUUCUUGAACUG | SS |
| nta-miR482d | 0.78 | $4.42 \times 10^{-4}$ | UUCCCGACUCCCCCCAUACCAC | SS |
| nta-miR6145a | −0.55 | $4.91 \times 10^{-2}$ | CAUUUUCACAUGUAGCACUGAC | SS |
| nta-miR6149a | 0.75 | $1.51 \times 10^{-3}$ | UUGAUACGCACCUGAAUCGGC | SS |
| miR-novel_31 | −0.93 | $4.56 \times 10^{-4}$ | AAGGACUGCUAUUUAGAAAUUAGC | SS |
| miR-novel_59 | −0.57 | $2.21 \times 10^{-2}$ | ACGGGCUGCUAUUUAAGAAUUAGC | SS |
| miR-novel_61 | 1.15 | $1.82 \times 10^{-5}$ | UUGAAGUGUUUGGGGGAACUC | SS |
| miR-novel_64 | −0.98 | $1.62 \times 10^{-3}$ | CUCCGGUCAAGAUCUUCCAUC | SS |
| miR-novel_127 | −0.71 | $3.30 \times 10^{-2}$ | ACGUGUCGGAUCCUCUAAAAGU | SS |
| miR-novel_163 | −0.81 | $1.48 \times 10^{-2}$ | AUGGCGUGGCUUCAGAUCUCUGAU | SS |
| miR-novel_216 | −1.86 | $3.39 \times 10^{-8}$ | AGGACGAUCUCUAUGACUCUUUGG | SS |
| miR-novel_228 | −0.88 | $9.24 \times 10^{-3}$ | ACGUGGACUGGGCUGGGCUAGCCU | SS |
| miR-novel_237 | −0.65 | $3.14 \times 10^{-2}$ | AGGACUGCUAUUUAGAAAUUAGGC | SS |
| miR-novel_258 | −0.84 | $7.63 \times 10^{-3}$ | ACUCCGAUUUGUGUAUGACUUGAC | SS |
| nta-miR156a | 0.71 | $2.82 \times 10^{-2}$ | UGACAGAAGAGAGUGAGCAC | AS |
| nta-miR164a | 0.84 | $2.40 \times 10^{-2}$ | UGGAGAAGCAGGGCACGUGCA | AS |
| nta-miR168a | 0.83 | $3.65 \times 10^{-4}$ | UCGCUUGGUGCAGGUCGGGAC | AS |
| nta-miR168d | 0.73 | $2.59 \times 10^{-2}$ | UCGCUUGGUGCAGGUCGGGAA | AS |
| nta-miR171c | 1.00 | $8.94 \times 10^{-3}$ | UGAUUGAGCCGUGCCAAUAUC | AS |
| nta-miR394 | 0.85 | $1.83 \times 10^{-2}$ | UUGGCAUUCUGUCCACCUCC | AS |
| nta-miR398 | −0.70 | $2.68 \times 10^{-2}$ | UGUGUUCUCAGGUCGCCCCUG | AS |
| nta-miR408 | −0.70 | $1.94 \times 10^{-2}$ | UGCACUGCCUCUUCCCUGGCU | AS |
| nta-miR482b-3p | 0.85 | $1.61 \times 10^{-2}$ | UCUUGCCAAUGCCAUCCAUUCC | AS |
| nta-miR6020b | 1.12 | $2.31 \times 10^{-3}$ | AAAUGUUCUUCGAGUAUCUUC | AS |
| nta-miR6145e | 0.54 | $4.90 \times 10^{-2}$ | AUUGUUACAUGUAGCCACUGGC | AS |
| nta-miR6149a | 0.69 | $2.27 \times 10^{-2}$ | UUGAUACGCACCUGAAUCGGC | AS |
| nta-miR6159 | 0.72 | $1.57 \times 10^{-2}$ | UAGCAUAGAAUUCUCGCACCUA | AS |
| nta-miR827 | 0.64 | $3.92 \times 10^{-2}$ | UUAGAUGAACAUCAACAAACA | AS |
| miR-novel_43 | −1.08 | $5.83 \times 10^{-5}$ | UUGGGCGUGCACAAGUAGGC | AS |
| miR-novel_64 | −1.17 | $1.38 \times 10^{-3}$ | CUCCGGUCAAGAUCUUCCAUC | AS |
| miR-novel_93 | 1.18 | $1.42 \times 10^{-3}$ | ACGCAGGAGAGAUGAUGCUGGA | AS |
| miR-novel_156 | −0.91 | $1.26 \times 10^{-2}$ | ACCGAUGUGGGACUCUGUCUAAAG | AS |
| miR-novel_167 | −0.91 | $9.95 \times 10^{-3}$ | AAAGAGCUCUAUAUAUAAAAAUGU | AS |
| miR-novel_193 | −0.81 | $2.60 \times 10^{-2}$ | AAGUCCGGUAACAUUUUGAAGAGU | AS |
| miR-novel_215 | −1.29 | $1.11 \times 10^{-4}$ | ACGUGGGCUGGGCUGAGCUAACCC | AS |
| miR-novel_216 | −1.31 | $4.12 \times 10^{-4}$ | AGGACGAUCUCUAUGACUCUUUGG | AS |

### 2.6. Integration Analysis of the miRNAs and mRNAs

The interaction between DE miRNAs and their targets was investigated using Cystoscape (version 3.6.1). A total of 165 miRNA-mRNA interactions were identified among the SS and AS treatments, with the involvement of 24 DE miRNAs and 158 DE mRNAs (Figure 4, Table S5). Figure 4 shows that a single miRNA can regulate multiple mRNAs and that a single mRNA can be targeted by more than one miRNA. These results suggest that the miRNA and mRNA interaction network involved

in salt and alkali stress is highly complex, especially for different miRNAs with their targets under various conditions.
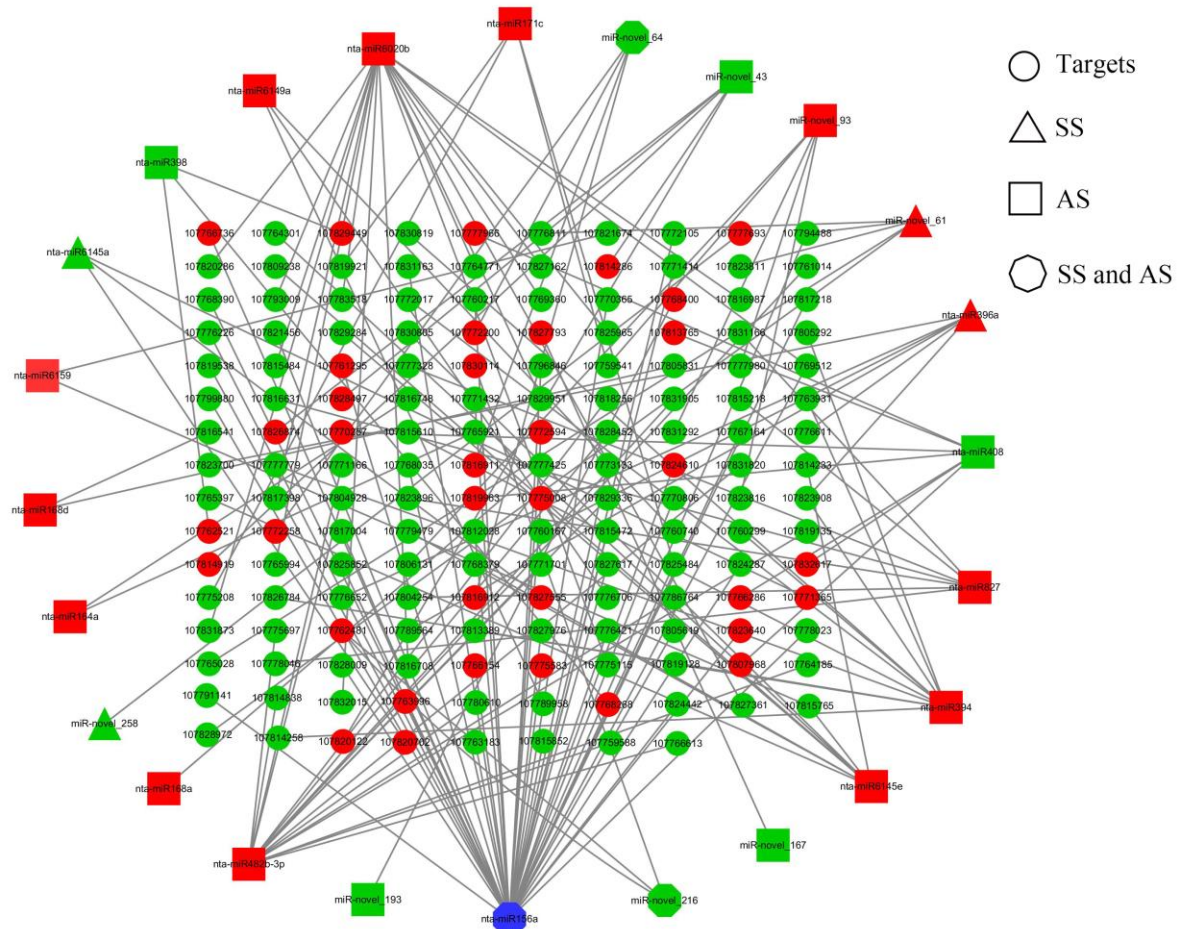


**Figure 4.** miRNA-mRNA correlation network. The circles in the network indicate the target mRNAs. The triangles, squares and octagons in the network indicate the DE miRNAs regulated by the SS, AS, and SS and AS treatments, respectively. Downregulated mRNAs and miRNAs are shown as green, and upregulated mRNAs and miRNAs are shown as red. Differential expression regulation by both SS and AS is shown in blue.

## 2.7. RT-qPCR Validation of DE mRNAs and miRNAs

To validate the mRNA and miRNA sequencing data, the expression levels of four DE miRNAs (nta-miR156a, nta-miR6149a, nta-miR394, nta-miR398) and eight DEGs (*CHX 15*, *AKT 1*, *ABCG 11*, *PIP 2-7*, *SOD*, *AMY*, *SUS2*, *RPP 13*), which were determined to be important for salt and alkali stress in our study, were manually selected and analyzed by RT-qPCR (Figure 5). As expected, with the exception of that of RPP 13 in the SS treatment, the expression patterns of most of the examined miRNAs and genes were similar, showing the accuracy and reliability of the RNA-seq data.
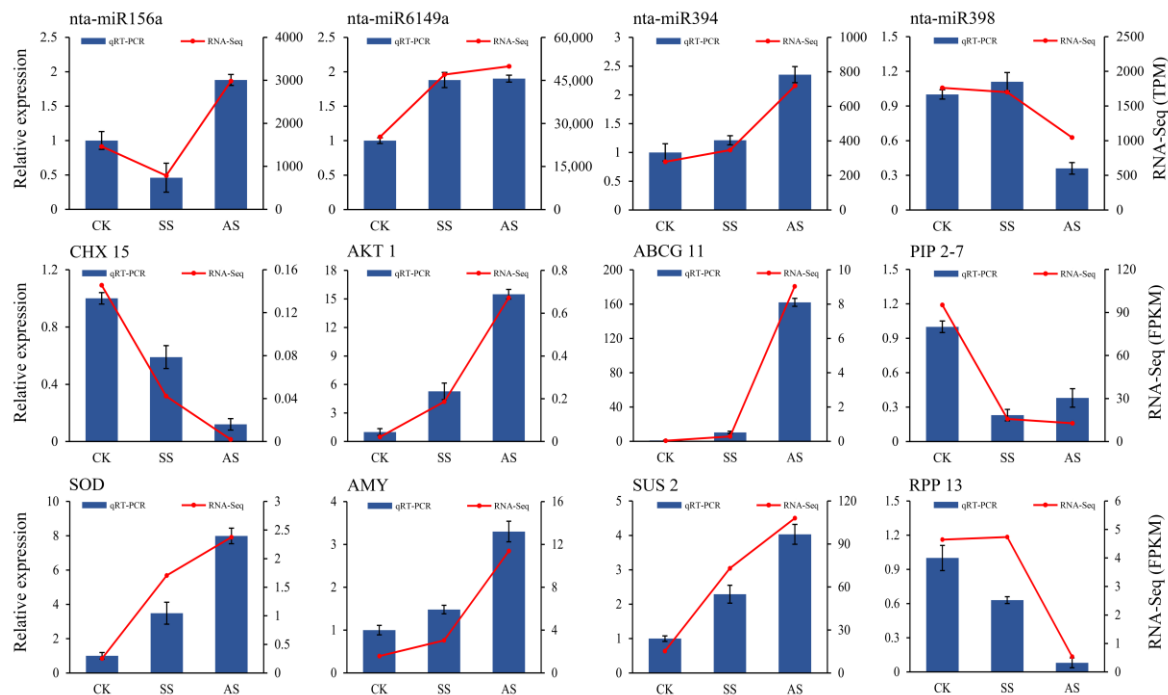
**Figure 5.** RT-qPCR analysis of miRNAs and mRNAs. The miRNAs and mRNAs were isolated from tobacco treated with NaCl (SS) and NaHCO3 (AS), respectively. The 5.8S rRNA and ef1α genes were chosen as the internal controls for miRNA and mRNA, respectively.

## 3. Discussion

As one of the most threatening environmental stress factors, salt-alkali stress can hinder plant growth and development in several ways. Accelerated NGS technology enables the investigation of a wide range of physiological and metabolic mechanisms of stress responses at the molecular level. In this study, we first conducted an integrative analysis of mRNA and miRNA expression levels in tobacco under salt and alkali stress. From this integrative analysis, we obtained a valuable set of salt-alkali-responsive mRNAs and miRNAs and identified the interactions and potential roles of these mRNAs and miRNAs in biophysiological processes between NaCl and NaHCO$_3$ treatments. These data provide a comprehensive understanding of the differences between salt and alkali stress response mechanisms.

### 3.1. mRNA Profiling in Leaves of Tobacco under Salt-Alkali Stress

Under salt-alkali stress, plants can accumulate essential substances for osmotic adjustment and can regulate gene expression levels to maintain ionic homeostasis [38]. Cation/H$^+$ antiporters (CHXs) operate as Na$^+$/H$^+$ antiporters or K$^+$/H$^+$ antiporters that help mediate biological responses to excess ions. For example, AtCHX17 is strongly induced by salt stress and is involved in K$^+$ acquisition [39]. Moreover, an appropriate K$^+$:Na$^+$ ratio in the cytoplasm is important for salt tolerance in plants. Overexpression of the potassium channel gene *OsKAT1* has been shown to enhance rice Na$^+$ tolerance by regulating K$^+$/Na$^+$ homeostasis [40]. In our study, the expression of three CHXs and AKT 1 significantly changed under SS and AS treatments (Table 4), suggesting that these ion transporters are responsible for tobacco resistance to salt toxicity via enhanced efflux of Na$^+$ and absorption of K$^+$. In addition, ABC transporters use energy from ATP hydrolysis for nutrient uptake and play an important role in ion homeostasis [41]. In our study, an increased abundance of ABCG11 but suppressed expression of ABCA7 were identified under both the SS and AS treatments (Table 4). Panikashvili et al. demonstrated that AtWBC11 (AtABCG11) is induced by salt and that wbc11 mutants are highly sensitive to salt stress [42], suggesting a potential role for this protein in plant salt tolerance.

**Table 4.** Candidate DEGs under SS and AS treatment.

| Gene ID | CK (FPKM) | SS (FPKM) | AS (FPKM) | Log$_2$FC (SS/CK) | Log$_2$FC (AS/CK) | Regulation | Annotation |
|---|---|---|---|---|---|---|---|
| Ion transport | | | | | | | |
| 107775281 | 0.13 | 0 | 0 | −inf | −inf | Down | cation/H(+) antiporter 18 |
| 107803899 | 0.02 | 0.18 | 0.13 | 3.05 | 2.46 | Up | cation/H(+) antiporter 15 |
| 107814619 | 0.02 | 0.19 | 0.67 | 2.83 | 4.61 | Up | potassium channel AKT1 |
| 107774409 | 0.04 | 0.28 | 9.04 | 2.68 | 7.62 | Up | ABC transporter G family member 11 |
| 107800765 | 1.53 | 0.40 | 0.20 | −2.22 | −3.26 | Down | ABC transporter B family member 19 |
| Aquaporins | | | | | | | |
| 107762778 | 12.65 | 1.79 | 1.38 | −3.12 | −3.56 | Down | aquaporin PIP2-1 |
| 107782948 | 42.89 | 6.99 | 6.57 | −2.92 | −3.07 | Down | aquaporin PIP2-1 |
| 107786743 | 39.82 | 7.32 | 4.89 | −2.74 | −3.39 | Down | aquaporin PIP2-7 |
| 107789972 | 95.21 | 15.78 | 12.69 | −2.89 | −3.27 | Down | aquaporin PIP2-7 |
| 107807226 | 75.86 | 8.04 | 6.26 | −3.54 | −3.96 | Down | aquaporin TIP1-3 |
| 107814785 | 34.86 | 2.09 | 2.89 | −4.36 | −3.95 | Down | aquaporin TIP2-1 |
| 107820018 | 31.08 | 7.70 | 6.70 | −2.31 | −2.58 | Down | aquaporin TIP1-3 |
| 107821662 | 4.55 | 1.28 | 0.39 | −2.13 | −3.92 | Down | aquaporin TIP2-1 |
| Antioxidant activity | | | | | | | |
| 107819573 | 0.08 | 0.48 | 0.71 | 2.23 | 2.74 | Up | superoxide dismutase family |
| 107832827 | 0.25 | 1.71 | 2.38 | 2.45 | 2.86 | Up | superoxide dismutase family |
| 107781013 | 2.73 | 17.09 | 16.50 | 2.34 | 2.23 | Up | catalase family |
| 107758994 | 1.20 | 0.11 | 0 | −3.74 | −inf | Down | peroxidase 19 |
| 107766849 | 0.28 | 0 | 0 | −inf | −inf | Down | peroxidase 10 |
| 107777661 | 0.40 | 3.98 | 2.17 | 3.04 | 2.08 | Up | peroxidase P7 |
| 107793453 | 0.48 | 3.42 | 5.06 | 2.56 | 3.05 | Up | peroxidase P7 |
| 107813838 | 0.24 | 2.62 | 1.34 | 3.17 | 2.13 | Up | peroxidase 12 |
| 107814038 | 0.14 | 0 | 0 | −inf | −inf | Down | peroxidase 3 |
| 107820597 | 0.81 | 4.34 | 5.04 | 2.13 | 2.28 | Up | probable glutathione peroxidase 8 |
| 107777621 | 6.99 | 40.69 | 87.80 | 2.24 | 3.29 | Up | glutathione transferase GST 23 |
| 107764067 | 1.12 | 14.98 | 74.03 | 3.44 | 5.68 | Up | glutathione transferase GST 23 |

Aquaporins (AQPs) are integral membrane proteins that regulate the transport of water and small molecules. In Arabidopsis and *Beta vulgaris*, the transcript abundance of most of the AQPs decreased in response to salt [43,44]. Hu et al. demonstrated that overexpression of the wheat AQP gene TaAQP8 increased salt stress tolerance in tobacco [45]. The expression levels of eight AQP genes in this study were consistent with previous results (Table 4), indicating that salt-alkali stress disrupts the balance of water transport efficiency [46].

Plant exposure to salt-alkali stress often generates ROS, which cause lipid peroxidation and DNA damage [47]. Plants can mediate the removal of ROS via antioxidant defense enzymes, including superoxide dismutase (SOD), catalase (CAT), peroxidase (POD) and glutathione S-transferase (GST) [48]. Our GO enrichment results indicated that DEGs were significantly enriched in the "antioxidant activity" term under both the SS and AS treatments. As expected, our experimental data showed that the expression of most of the ROS-scavenging enzymes, including SOD, CAT, POD, glutathione peroxidase (GR) and GST, was upregulated under salt-alkali treatment (Table 4), indicating that these scavenging enzymes have active functions that provide resistance to salt and alkali stress in tobacco.

Photosynthesis is a well-studied primary metabolic process that is affected by environmental stress. The response of plant photosynthesis to salinity is typically accompanied by stomal closure, reduced $CO_2$ diffusion into chloroplasts and alterations in leaf photochemistry [6]. KEGG pathway analysis indicated that DEGs were significantly enriched in "photosynthesis-antenna proteins" under salt-alkali treatment but were enriched in only "photosynthesis" in AS-treated samples. As shown in Figure 6, the transcript abundance of genes involved in the photosynthetic process decreased. Under salt-alkali stress, DEGs encoding light-harvesting complexes, such as Lhca in photosystem I (PSI) and Lhcb in photosystem II (PSII), was downregulated (Figure 6A), suggesting that the capture of light energy was restricted by the SS and AS treatments. Photo-oxidation of water in plants is accomplished by the oxygen-evolving complex of PSII. The decreased abundance of the genes encoding this complex, including PsbO, PsbP, PsbQ, PsbS, PsbY and Psb27, may inhibit the oxygen-evolving capacity of PSII for water oxidation (Figure 6B). Furthermore, the similar expression profiles of DEGs encoding electron

transport proteins and ATP synthase indicated an inhibitory effect on the mechanism of electron transport and resulted in the inhibition of ATP synthesis under AS treatment. Taken together, our experimental data revealed that NaHCO₃ stress strongly affects the process of photosynthesis because of the marked decrease in the expression levels of a wide range of relevant genes.
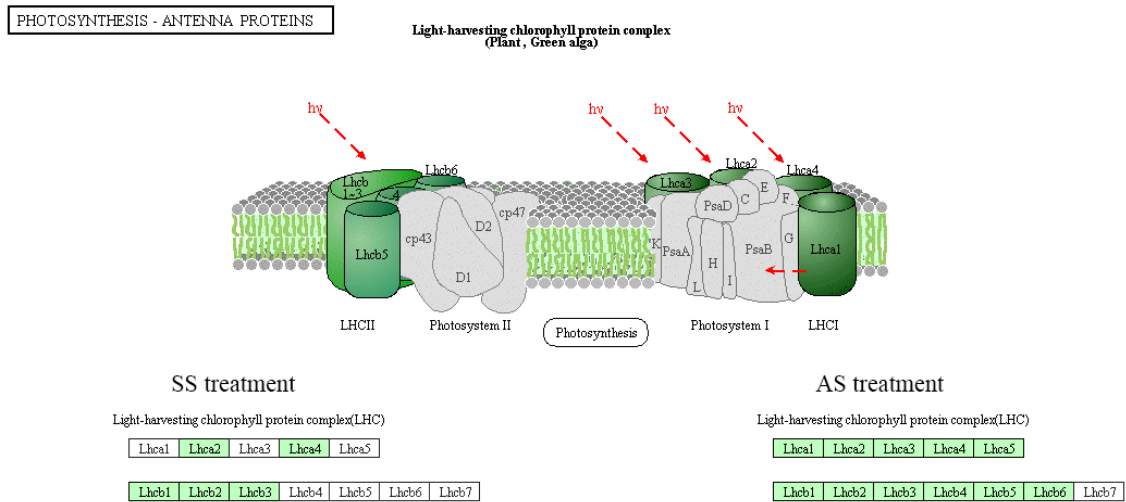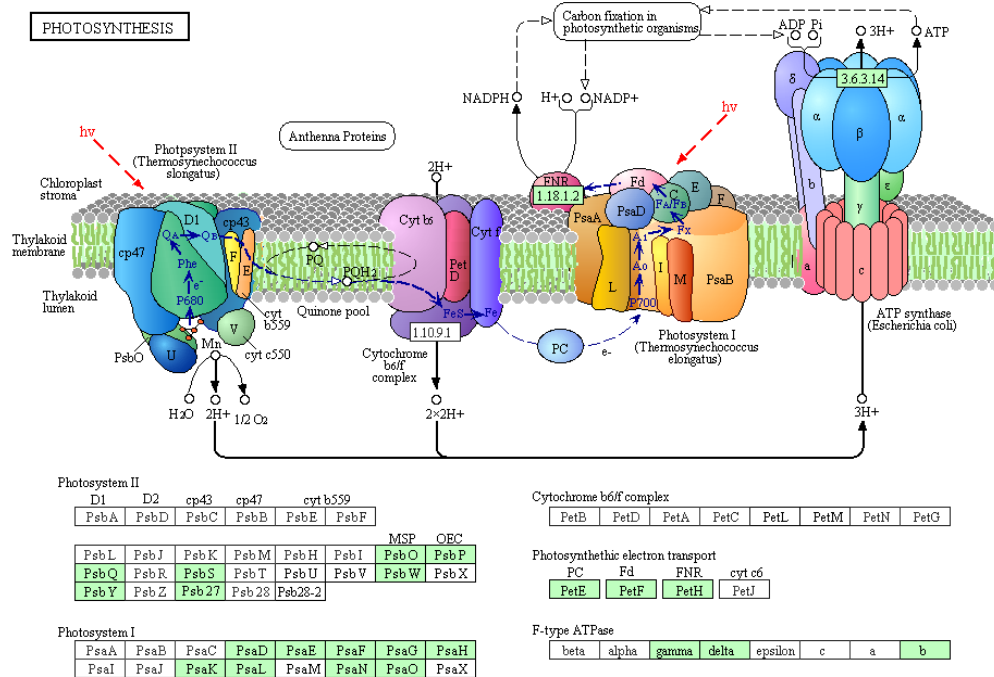


**Figure 6.** Summary of gene expression related to the photosynthetic machinery in response to SS and AS. KEGG maps of the "photosynthesis-antenna proteins" (**A**) and "photosynthesis" (**B**) pathways are displayed. The green boxes indicate expression levels of the corresponding genes that were downregulated.

Soluble carbohydrates can promptly accumulate in plants to cope with various forms of abiotic stress. Starch is the predominant carbohydrate storage material that is synthesized by plants. Our KEGG pathway enrichment analysis revealed that the DEGs were markedly enriched in the "starch and sucrose metabolism" pathway under AS treatment but not under SS treatment. Granule-bound

starch synthase (GBSS) catalyzes the synthesis of starch, while α-amylase (AMY) and β-amylase (BMY) are responsible for degrading plant starch. Numerous studies have revealed significant changes in the expression levels of GBSS, AMY and BMY under various forms of abiotic stress [49,50]. Similarly, the expression of GBSS 1 was downregulated by $NaHCO_3$ treatment, but that of AMY and BMY was upregulated (Figure 7). Zhang et al. reported that the transcript abundance of genes encoding sucrose synthase (Sus) increased under high-pH stress (NaOH treatment). Consistent with this observation, the induction of Sus2 genes by AS in our study may be responsible for high-pH-induced oxygen deficiency conditions, as Sus2 was induced specifically by oxygen deficiency [51]. Trehalose is a non-reducing disaccharide that serves as an energy source for plants subjected to stress [52]. Trehalose-6-phosphate synthase (TPS) is a key enzyme involved in the biosynthesis of trehalose. In our study, we found that the expression of three genes encoding the TPS enzyme was induced and that the expression of only one TPS was downregulated by AS (Figure 7). Taken together, the results show that enhancement of starch and sucrose metabolism may provide energy requirements for tobacco resistance to $NaHCO_3$-induced osmotic stress.
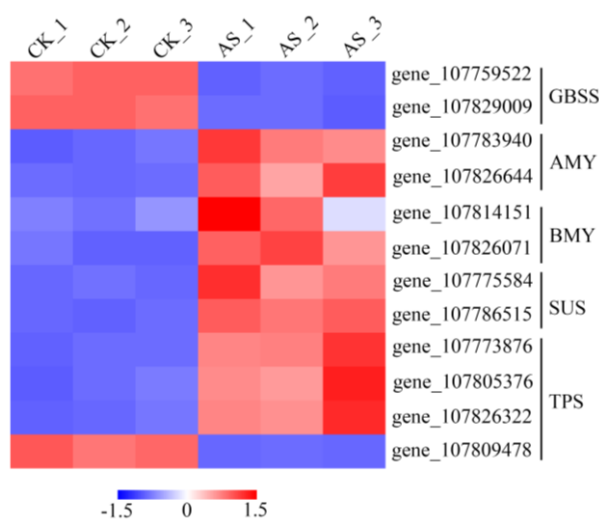


**Figure 7.** Heatmap of specifically expressed genes related to the "starch and sucrose metabolism" pathway in the AS treatment.

## 3.2. miRNA Profiling of the Salt-Alkali Response in Tobacco

Numerous recent studies have demonstrated that miRNAs play crucial roles in plant growth and development and in the plant responses to adverse environmental stress. In our study, we performed sRNA sequencing on the CK, SS and AS samples and identified 89 known miRNAs from 52 families and 102 novel miRNAs. Consistent with the results of a previous sRNA sequencing study in tobacco [33], our results showed that the most abundant transcript was that of nta-miR166a, followed by nta-miR159, nta-miR6149a and nta-miR6021, across the nine libraries (Table S4).

Many miRNAs are closely associated with salt-alkali stress in various plant species, such as Arabidopsis [53], radish [54], flax [55] and *Medicago truncatula* [56]. In the present study, 17 known miRNAs and 16 novel miRNAs were found to respond to salt-alkali stress in tobacco. We detected significant regulation of the miR156, miR482, miR6145 and miR6149 families under both salt and alkali stress. The conserved miR156 family is one of the most well-studied plant miRNA families and plays a vital role in plant stress responses, including salt-alkali resistance in alfalfa [57], cotton [58] and *Populus euphratica* [59]. The roles of miR482 in drought and cold stress, miR6145 in the wound response and miR6149 in Cr stress were also investigated [60–63]. Our experimental data confirmed the significance of miR156 in tobacco under salt-alkali conditions and provide valuable information concerning the roles of miR482, miR6145 and miR6149 in the response to salt-alkali stress. Notably, two of these overlapping miRNA families, namely, miR156 (nta-miR156a) and miR6145 (nta-miR6145a/e),

exhibited differential regulation upon exposure to NaCl and NaHCO$_3$ stress in our experiment. A similar result for miR156 was obtained in a previous study, which revealed that the expression of miR156 was downregulated after 4 h [64] but upregulated after 72 h of salt treatment in Medicago [56].

In addition to these four overlapping miRNA families, eight upregulated miRNAs (including nta-miR164a, nta-miR168a, nta-miR168d, nta-miR171c, nta-miR394) and two downregulated miRNAs (nta-miR398, nta-miR408) were markedly expressed under NaHCO$_3$ stress, and nta-miR396a was specifically upregulated by NaCl. Liu et al. reported that miR168, miR171 and miR394 were induced and that miR398 was suppressed by salt stress in Arabidopsis [53]. Sun et al. demonstrated that the expression of miR164a and miR396a-3p was upregulated and that the expression of miR398b-3p was downregulated under salt stress in *Raphanus sativus* L. [54]. As miRNAs are evolutionarily conserved between plant species, our work here indicated the occurrence of miRNA regulation in tobacco under salt-alkali stress. Moreover, 16 novel salt-alkali-responsive miRNAs were identified, and the structural precursors of these novel miRNAs are presented in Figure S2. However, further validation is needed to confirm the authenticity of such novel miRNAs accurately.

In general, miRNAs negatively regulate gene transcription levels by target RNA cleavage based on sequence complementarity with targets. Our integrated analysis of miRNA and mRNA transcript levels revealed inverse regulation of 26 and 139 miRNA-mRNA interactions in the SS and AS treatments, respectively. For instance, the miR156 target squamosa promoter-binding protein like (SPL), which plays a role in flower regulation and reproductive growth [65], was also identified in our study. Recently, a role for the miR156/SPL network in the regulation of the content of ROS and salicylic acid (SA) signal transduction was identified in Arabidopsis [66]. As expected, nt-miR156a-targeted SPL members exhibited strict negative regulation in both the SS and AS treatments, suggesting that nt-miR156a plays an important role in salt-alkali stress by regulating the expression of SPLs. Nucleotide-binding sites and leucine-rich repeat (NBS-LRR) regions constitute the main components of disease resistance proteins [67]. These NBS-LRR proteins function in the plant response to pathogenic infection. Interestingly, nt-miR482b-targeted NBS-LRR proteins were identified in our AS treatment, suggesting that this previously verified regulatory mode may also be involved in alkali stress because plants can employ multiple stress response pathways to cope with environmental stress [68–70].

Additionally, a large number of salt or alkali stress-responsive DE miRNAs and their targets, such as nta-miR396a/U-BOX, nta-miR408/NAC domain, nta-miR482b-3p/NB-ARC domain, nta-miR6145e/leucine-rich repeat protein kinase, nta-miR6149a/F-BOX and miR-novel_93/Dof domain protein, which may provide salt and alkali stress tolerance, were predicted in our study (Table S5); however, the interactions in this regulatory network need to be further studied.

## 4. Materials and Methods

### 4.1. Plant Materials and Salt-Alkali Treatment

*N. tabacum* ecotype K326 used in this study was obtained from Henan Agricultural University. Tobacco seeds were first sterilized in 75% ethanol for 10 min, rinsed with distilled water three times and then transferred to Murashige and Skoog (MS) medium. After approximately two weeks, germinated seedlings in the MS medium were transferred to plastic pots filled with Hoagland nutrient solution and cultivated in a phytotron under normal conditions (26 °C with 14 h days, 24 °C with 8 h nights, and 70% relative humidity). Tobacco plants grown to the five-leaf stage were used in this study. For salt stress treatment, seedlings were transferred to distilled water supplemented with 100 mM NaCl (pH = 7.0). For alkali stress, seedlings were transferred to distilled water supplemented with 100 mM NaHCO$_3$ (pH = 8.4). After they were exposed to the stress treatment for 24 h, the samples were harvested, frozen in liquid nitrogen and then stored at −80°C.

*4.2. Construction and Sequencing of mRNA-seq and sRNA Libraries*

Total RNA was extracted from tobacco leaves using TRIzol reagent (Invitrogen, Carlsbad, CA, USA). The concentration and quality of the RNA samples were assessed using a Nanodrop 2000 instrument (Thermo, Waltham, MA, USA). mRNA-seq libraries were established using an Illumina TruSeq RNA Sample Prep Kit (Illumina, San Diego, CA, USA) according to the manufacturer's protocol [71]. Briefly, 5 μg of mRNA was isolated from the total RNA using oligo (dT) magnetic beads (Invitrogen, Carlsbadcity, CA, USA), fragmented and reverse transcribed into cDNA. Adapters with a hairpin loop structure were ligated to cDNA molecules and amplified by PCR. The RNA-seq library was sequenced using the Illumina HiSeq X Ten platform (Illumina, San Diego, CA, USA). For small RNA (sRNA) sequencing, RNA bands of approximately 18–30 nt were isolated, linked to 5′ and 3′ adapters and reverse transcribed to cDNA. The final PCR products were purified and sequenced with the Illumina HiSeq 2500 sequencing platform (Illumina, San Diego, CA, USA) with 50-bp single-end reads.

*4.3. Mapping of mRNA-seq Reads*

To obtain clean reads, adapters and low-quality sequence reads were removed from the raw data using Trimmomatic (version 0.30) [72]. These clean reads were mapped to the tobacco genome (available online: ftp://ftp.solgenomics.net/genomes/Nicotiana_tabacum/) using HISAT2 (version 2.0.5) [73]. The gene expression levels in all nine libraries were presented as fragments per kilobase of transcript per million (FPKM) [74].

*4.4. Analysis of Differential Gene Expression in Response to Salt-Alkali Stress*

DEG analysis was carried out using the DESeq R package (1.10.1). Using a model based on the negative binomial distribution, this tool provides statistical routines for determining differential expression within digital gene expression data. On the basis of this method, genes with $|\log_2 FC|>2$ and a $p$-value $< 0.05$ were classified as DEGs between two comparisons among the three experimental conditions.

*4.5. GO and KEGG Pathway Enrichment Analysis*

GO enrichment analysis of the DEGs was carried out using the GOseq R package with the default parameters, by which gene length bias was corrected [75]. The KEGG database is a widely used resource for understanding high-level functions and utilities of biological systems (available online: http://www.genome.jp/kegg/). The DEGs in the KEGG pathways were analyzed using KOBAS (version 2.0) [76].

*4.6. Identification of Known and Novel miRNAs and Prediction of miRNA Targets*

After the adapter sequences, poly-A sequences and low-quality bases were removed from the raw reads, the remaining unique sequences were mapped to the tobacco genome using Bowtie2 (version 2.0.5) [73]. The sRNA sequences that matched those of rRNA, tRNA, small nuclear RNA (snRNA) and small nucleolar RNA (snoRNA) were excluded. The remaining unique sequences were searched against miRBase 20.0 to identify known miRNAs in tobacco. The software programs miREvo [77] and mirdeep2 [78] were used to predict novel miRNAs and to explore secondary structures, and the miRNA targets were predicted using psRobot [79].

*4.7. Detection of the Differential Expression of miRNAs in Response to Salt-Alkali Stress*

The evaluation of the differential expression of miRNAs between two comparable groups was based on a previously established model [80]. Using $|\log_2 FC|>0.5$ and $p$-value $< 0.05$ as criteria, we adjusted for multiple testing to classify the DE miRNAs among the three experimental conditions.

*4.8. Validation of mRNA and miRNA Expression*

Total RNA was extracted from each treatment using TRIzol reagent (Invitrogen, USA) as described above. cDNA was generated using a PrimeScript cDNA Synthesis Kit (Takara, Dalian, China) according to the manufacturer's instructions and then diluted 10 times for use as a qPCR template. sRNA was extracted using a Small RNA Isolation Kit (Takara, Dalian, China). RT-qPCR was performed using SYBR Green Supermix (Takara, Dalian, China) on an ABI StepOne instrument. The tobacco ef1$\alpha$ gene was used as an internal control for mRNA analysis, and 5.8S rRNA was used as the reference for stem-loop miRNA analysis. Three independent biological replicates were included in the qRT-PCR analyses. The relative expression level of each sample was calculated using the $2^{-\Delta\Delta CT}$ method [81]. The primers used for this RT-qPCR experiment are listed in Table S6.

## 5. Conclusions

In the present study, we comprehensively analyzed the changes in the mRNA and sRNA profiles of tobacco under NaCl and NaHCO$_3$ treatment. Overall, 8064 mRNAs and 33 miRNAs were differentially expressed in response to salt and alkali stress. The overlapping DEGs between the two treatments suggested that plants could utilize similar strategies, such as ion channels, AQPs and antioxidant activity, to adapt to both NaCl and NaHCO$_3$ stress. However, our GO and KEGG pathway enrichments revealed that many essential biological processes, including "photosynthesis" and "starch and sucrose metabolism," were specifically enriched in the NaHCO$_3$ treatment. In addition, our analysis also revealed many miRNAs, including four overlapping miRNA families, that might play important roles in the response of tobacco to salt and alkali stress. Several inverse regulatory processes of miRNAs with their target transcript genes were also predicted for manipulation. These findings improve our understanding of the underlying salt and alkali responses in tobacco at the molecular level and provide a valuable foundation for future uses of the miRNA-based genetic regulatory network in breeding for salinity tolerance in crops.

**Supplementary Materials:** Supplementary File 1. Supplementary materials can be found at http://www.mdpi.com/1422-0067/20/10/2391/s1.

**Author Contributions:** Conceptualization, Z.X. and J.X.; methodology, Z.X., J.X., Q.C. and P.L.; software, J.X., Q.C. and W.J.; writing—original draft preparation, J.X.; writing—reviewing and editing, Z.X., J.X., Q.C., P.L., W.J. and Z.C.; Supervision, Z.X.

**Conflicts of Interest:** The authors declare no conflict of interest.

## References

1. Munns, R.; Tester, M. Mechanisms of salinity tolerance. *Annu. Rev. Plant Biol.* **2008**, *59*, 651–681.
2. Zhang, B.; Chen, X.; Lu, X.; Shu, N.; Wang, X.; Yang, X.; Wang, S.; Wang, J.; Guo, L.; Wang, D.; et al. Transcriptome Analysis of Gossypium hirsutum L. Reveals Different Mechanisms among NaCl, NaOH and Na$_2$CO$_3$ Stress Tolerance. *Sci. Rep.* **2018**, *8*, 13527. [CrossRef]
3. Razzaghi, F.; Jacobsen, S.-E.; Jensen, C.R.; Andersen, M.N. Ionic and photosynthetic homeostasis in quinoa challenged by salinity and drought—Mechanisms of tolerance. *Funct. Plant Biol.* **2015**, *42*, 136–148. [CrossRef]
4. Gupta, B.; Huang, B. Mechanism of Salinity Tolerance in Plants: Physiological, Biochemical, and Molecular Characterization. *Int. J. Genom.* **2014**. [CrossRef]
5. Hagemann, M. Molecular biology of cyanobacterial salt acclimation. *Fems Microbiol. Rev.* **2011**, *35*, 87–123. [CrossRef]
6. Aghaei, K.; Ehsanpour, A.A.; Komatsu, S. Potato Responds to Salt Stress by Increased Activity of Antioxidant Enzymes. *J. Integr. Plant Biol.* **2009**, *51*, 1095–1103. [CrossRef] [PubMed]
7. Chinnusamy, V.; Jagendorf, A.; Zhu, J.K. Understanding and improving salt tolerance in plants. *Crop Sci.* **2005**, *45*, 437–448. [CrossRef]

8.  Tang, J.; Liu, Q.Q.; Yuan, H.Y.; Zhang, Y.X.; Huang, S.Z. Molecular analysis of a novel alkaline metal salt (NaCl)-responsive WRKY transcription factor gene IlWRKY1 from the halophyte Iris lactea var. chinensis. *Int. Biodeterior. Biodegrad.* **2018**, *127*, 139–145. [CrossRef]

9.  Budak, H.; Akpinar, B.A. Plant miRNAs: Biogenesis, organization and origins. *Funct. Integr. Genom.* **2015**, *15*, 523–531. [CrossRef] [PubMed]

10. Sunkar, R.; Li, Y.-F.; Jagadeeswaran, G. Functions of microRNAs in plant stress responses. *Trends Plant Sci.* **2012**, *17*, 196–203. [CrossRef] [PubMed]

11. Xie, R.; Zhang, J.; Ma, Y.; Pan, X.; Dong, C.; Pang, S.; He, S.; Deng, L.; Yi, S.; Zheng, Y.; et al. Combined analysis of mRNA and miRNA identifies dehydration and salinity responsive key molecular players in citrus roots. *Sci. Rep.* **2017**, *7*. [CrossRef]

12. Shenoy, A.; Blelloch, R.H. Regulation of microRNA function in somatic stem cell proliferation and differentiation. *Nat. Rev. Mol. Cell Biol.* **2014**, *15*, 565–576. [CrossRef]

13. Gao, R.; Wang, Y.; Gruber, M.Y.; Hannoufa, A. miR 156/SPL10 Modulates Lateral Root Development, Branching and Leaf Morphology in Arabidopsisby Silencing AGAMOUS-LIKE 79. *Front. Plant Sci.* **2018**, *8*. [CrossRef]

14. Cagirici, H.B.; Biyiklioglu, S.; Budak, H. Assembly and Annotation of Transcriptome Provided Evidence of miRNA Mobility between Wheat and Wheat Stem Sawfly. *Front. Plant Sci.* **2017**, *8*, 14. [CrossRef]

15. Poethig, R.S. Small RNAs and developmental timing in plants. *Curr. Opin. Genet. Dev.* **2009**, *19*, 374–378. [CrossRef]

16. Hu, J.-Y.; Zhou, Y.; He, F.; Dong, X.; Liu, L.-Y.; Coupland, G.; Turck, F.; de Meaux, J. miR824-Regulated AGAMOUS-LIKE16 Contributes to Flowering Time Repression in Arabidopsis. *Plant Cell* **2014**, *26*, 2024–2037. [CrossRef] [PubMed]

17. Hajyzadeh, M.; Turktas, M.; Khawar, K.M.; Unver, T. miR408 overexpression causes increased drought tolerance in chickpea. *Gene* **2015**, *555*, 186–193. [CrossRef]

18. Giusti, L.; Mica, E.; Bertolini, E.; De Leonardis, A.M.; Faccioli, P.; Cattivelli, L.; Crosatti, C. microRNAs differentially modulated in response to heat and drought stress in durum wheat cultivars with contrasting water use efficiency. *Funct. Integrative Genom.* **2017**, *17*, 293–309. [CrossRef]

19. Zhou, X.; Wang, G.; Sutoh, K.; Zhu, J.-K.; Zhang, W. Identification of cold-inducible microRNAs in plants by transcriptome analysis. *Biochimica Et Biophysica Acta-Gene Regulatory Mechanisms* **2008**, *1779*, 780–788. [CrossRef] [PubMed]

20. Xie, F.; Stewart, C.N., Jr.; Taki, F.A.; He, Q.; Liu, H.; Zhang, B. High-throughput deep sequencing shows that microRNAs play important roles in switchgrass responses to drought and salinity stress. *Plant Biotechnol. J.* **2014**, *12*, 354–366. [CrossRef] [PubMed]

21. Au, K.F.; Underwood, J.G.; Lee, L.; Wong, W.H. Improving PacBio Long Read Accuracy by Short Read Alignment. *PLoS ONE* **2012**, *7*, 8. [CrossRef] [PubMed]

22. Zhang, F.; Zhu, G.Z.; Du, L.; Shang, X.G.; Cheng, C.Z.; Yang, B.; Hu, Y.; Cai, C.P.; Guo, W.Z. Genetic regulation of salt stress tolerance revealed by RNA-Seq in cotton diploid wild species, Gossypium davidsonii. *Sci. Rep.* **2016**, *6*, 15. [CrossRef]

23. Takahashi, F.; Tilbrook, J.; Trittermann, C.; Berger, B.; Roy, S.J.; Seki, M.; Shinozaki, K.; Tester, M. Comparison of Leaf Sheath Transcriptome Profiles with Physiological Traits of Bread Wheat Cultivars under Salinity Stress. *PLoS ONE* **2015**, *10*, 23. [CrossRef] [PubMed]

24. Fan, X.D.; Wang, J.Q.; Yang, N.; Dong, Y.Y.; Liu, L.; Wang, F.W.; Wang, N.; Chen, H.; Liu, W.C.; Sun, Y.P.; et al. Gene expression profiling of soybean leaves and roots under salt, saline-alkali and drought stress by high-throughput Illumina sequencing. *Gene* **2013**, *512*, 392–402. [CrossRef]

25. Negrao, S.; Almadanim, M.C.; Pires, I.S.; Abreu, I.A.; Maroco, J.; Courtois, B.; Gregorio, G.B.; McNally, K.L.; Oliveira, M.M. New allelic variants found in key rice salt-tolerance genes: An association study. *Plant Biotechnol. J.* **2013**, *11*, 87–100. [CrossRef] [PubMed]

26. Xie, R.J.; Pan, X.T.; Zhang, J.; Ma, Y.Y.; He, S.L.; Zheng, Y.Q.; Ma, Y.T. Effect of salt-stress on gene expression in citrus roots revealed by RNA-seq. *Funct. Integr. Genom.* **2018**, *18*, 155–173. [CrossRef]

27. Long, R.C.; Li, M.N.; Li, X.; Gao, Y.L.; Zhang, T.J.; Sun, Y.; Kang, J.M.; Wang, T.H.; Cong, L.L.; Yang, Q.C. A Novel miRNA Sponge Form Efficiently Inhibits the Activity ofmiR393 and Enhances the Salt Tolerance and ABA Insensitivity in Arabidopsis thaliana. *Plant Mol. Biol. Rep.* **2017**, *35*, 409–415. [CrossRef]

28. Feng, K.W.; Nie, X.J.; Cui, L.C.; Deng, P.C.; Wang, M.X.; Song, W.N. Genome-Wide Identification and Characterization of Salinity Stress-Responsive miRNAs in Wild Emmer Wheat (Triticum turgidum ssp dicoccoides). *Genes* **2017**, *8*, 18. [CrossRef]

29. Li, Y.S.; Li, C.H.; Bai, L.Q.; He, C.X.; Yu, X.C. MicroRNA and target gene responses to salt stress in grafted cucumber seedlings. *Acta Physiol. Plant.* **2016**, *38*, 12. [CrossRef]

30. Deng, P.C.; Wang, L.; Cui, L.C.; Feng, K.W.; Liu, F.Y.; Du, X.H.; Tong, W.; Nie, X.J.; Ji, W.Q.; Weining, S. Global Identification of MicroRNAs and Their Targets in Barley under Salinity Stress. *PLoS ONE* **2015**, *10*, 20. [CrossRef]

31. Fu, R.; Zhang, M.; Zhao, Y.C.; He, X.C.; Ding, C.Y.; Wang, S.K.; Feng, Y.; Song, X.L.; Li, P.; Wang, B.H. Identification of Salt Tolerance-related microRNAs and Their Targets in Maize (Zea mays L.) Using High-throughput Sequencing and Degradome Analysis. *Front. Plant Sci.* **2017**, *8*, 13. [CrossRef]

32. Yu, M.; Zhao, J. The cytological changes of tobacco zygote and proembryo cells induced by beta-glucosyl Yariv reagent suggest the involvement of arabinogalactan proteins in cell division and cell plate formation. *BMC Plant Biol.* **2012**, *12*, 16. [CrossRef]

33. Yin, F.; Gao, J.; Liu, M.; Qin, C.; Zhang, W.; Yang, A.; Xia, M.; Zhang, Z.; Shen, Y.; Lin, H.; et al. Genome-wide analysis of Water-stress-responsive microRNA expression profile in tobacco roots. *Funct. Integrative Genom.* **2014**, *14*, 319–332. [CrossRef]

34. Sierro, N.; Battey, J.N.D.; Ouadi, S.; Bakaher, N.; Bovet, L.; Willig, A.; Goepfert, S.; Peitsch, M.C.; Ivanov, N.V. The tobacco genome sequence and its comparison with those of tomato and potato. *Nat. Commun.* **2014**, *5*, 9. [CrossRef]

35. Bombarely, A.; Rosli, H.G.; Vrebalov, J.; Moffett, P.; Mueller, L.A.; Martin, G.B. A Draft Genome Sequence of Nicotiana benthamiana to Enhance Molecular Plant-Microbe Biology Research. *Mol. Plant-Microbe Interact.* **2012**, *25*, 1523–1530. [CrossRef]

36. Frazier, T.P.; Sun, G.L.; Burklew, C.E.; Zhang, B.H. Salt and Drought Stresses Induce the Aberrant Expression of microRNA Genes in Tobacco. *Mol. Biotechnol.* **2011**, *49*, 159–165. [CrossRef]

37. Aysin, F.; Erson-Bensan, A.; Eyidogan, F.; Oktem, H.A. Generating salt-tolerant Nicotiana tabacum and identification of stress-responsive miRNAs in transgenics. *Turk. J. Bot.* **2015**, *39*, 757–768. [CrossRef]

38. Yang, Y.; Guo, Y. Elucidating the molecular mechanisms mediating plant salt-stress responses. *New Phytologist* **2018**, *217*, 523–539. [CrossRef]

39. Cellier, F.; Conejero, G.; Ricaud, L.; Luu, D.T.; Lepetit, M.; Gosti, F.; Casse, F. Characterization of AtCHX17, a member of the cation/H$^+$ exchangers, CHX family, from Arabidopsis thaliana suggests a role in K+ homeostasis. *Plant J.* **2004**, *39*, 834–846. [CrossRef]

40. Obata, T.; Kitamoto, H.K.; Nakamura, A.; Fukuda, A.; Tanaka, Y. Rice Shaker potassium channel OsKAT1 confers tolerance to salinity stress on yeast and rice cells. *Plant Physiol.* **2007**, *144*, 1978–1985. [CrossRef]

41. Trowitzsch, S.; Tempe, R. ABC Transporters in Dynamic Macromolecular Assemblies. *J. Mol. Biol.* **2018**, *430*, 4481–4495. [CrossRef]

42. Panikashvili, D.; Savaldi-Goldstein, S.; Mandel, T.; Yifhar, T.; Franke, R.B.; Hoefer, R.; Schreiber, L.; Chory, J.; Aharoni, A. The Arabidopsis DESPERADO/AtWBC11 transporter is required for cutin and wax secretion. *Plant Physiol.* **2007**, *145*, 1345–1360. [CrossRef]

43. Afzal, Z.; Howton, T.C.; Sun, Y.L.; Mukhtar, M.S. The Roles of Aquaporins in Plant Stress Responses. *J. Dev. Biol.* **2016**, *4*. [CrossRef]

44. Kong, W.L.; Yang, S.Z.; Wang, Y.L.; Bendahmane, M.; Fu, X.P. Genome-wide identification and characterization of aquaporin gene family in Beta vulgaris. *Peerj* **2017**, *5*. [CrossRef]

45. Hu, W.; Yuan, Q.Q.; Wang, Y.; Cai, R.; Deng, X.M.; Wang, J.; Zhou, S.Y.; Chen, M.J.; Chen, L.H.; Huang, C.; et al. Overexpression of a Wheat Aquaporin Gene, TaAQP8, Enhances Salt Stress Tolerance in Transgenic Tobacco. *Plant Cell Physiol.* **2012**, *53*, 2127–2141. [CrossRef]

46. Lienard, D.; Durambur, G.; Kiefer-Meyer, M.C.; Nogue, F.; Menu-Bouaouiche, L.; Charlot, F.; Gomord, V.; Lassalles, J.P. Water transport by aquaporins in the extant plant Physcomitrella patens. *Plant Physiol.* **2008**, *146*, 1207–1218. [CrossRef] [PubMed]

47. Islam, F.; Yasmeen, T.; Riaz, M.; Arif, M.S.; Ali, S.; Raza, S.H. Proteus mirabilis alleviates zinc toxicity by preventing oxidative stress in maize (Zea mays) plants. *Ecotox. Environ. Saf.* **2014**, *110*, 143–152. [CrossRef] [PubMed]

48. Liang, C.Z.; Zheng, G.Y.; Li, W.Z.; Wang, Y.Q.; Hu, B.; Wang, H.R.; Wu, H.K.; Qian, Y.W.; Zhu, X.G.; Tan, D.X.; et al. Melatonin delays leaf senescence and enhances salt stress tolerance in rice. *J. Pineal Res.* **2015**, *59*, 91–101. [CrossRef] [PubMed]

49. Valerio, C.; Costa, A.; Marri, L.; Issakidis-Bourguet, E.; Pupillo, P.; Trost, P.; Sparla, F. Thioredoxin-regulated beta-amylase (BAM1) triggers diurnal starch degradation in guard cells, and in mesophyll cells under osmotic stress. *J. Exp. Bot.* **2011**, *62*, 545–555. [CrossRef]

50. Timabud, T.; Yin, X.J.; Pongdontri, P.; Komatsu, S. Gel-free/label-free proteomic analysis of developing rice grains under heat stress. *J. Proteomics* **2016**, *133*, 1–19. [CrossRef]

51. Dejardin, A.; Sokolov, L.N.; Kleczkowski, L.A. Sugar/osmoticum levels modulate differential abscisic acid-independent expression of two stress-responsive sucrose synthase genes in Arabidopsis. *Biochem. J.* **1999**, *344*, 503–509. [CrossRef]

52. Islam, M.O.; Kato, H.; Shima, S.; Tezuka, D.; Matsui, H.; Imai, R. Functional identification of a rice trehalase gene involved in salt stress tolerance. *Gene* **2019**, *685*, 42–49. [CrossRef]

53. Liu, H.-H.; Tian, X.; Li, Y.-J.; Wu, C.-A.; Zheng, C.-C. Microarray-based analysis of stress-regulated microRNAs in Arabidopsis thaliana. *RNA* **2008**, *14*, 836–843. [CrossRef]

54. Sun, X.; Xu, L.; Wang, Y.; Yu, R.; Zhu, X.; Luo, X.; Gong, Y.; Wang, R.; Limera, C.; Zhang, K.; et al. Identification of novel and salt-responsive miRNAs to explore miRNA-mediated regulatory network of salt stress response in radish (Raphanus sativus L.). *BMC Genom.* **2015**, *16*, 197. [CrossRef]

55. Yu, Y.; Wu, G.; Yuan, H.; Cheng, L.; Zhao, D.; Huang, W.; Zhang, S.; Zhang, L.; Chen, H.; Zhang, J.; et al. Identification and characterization of miRNAs and targets in flax (Linum usitatissimum) under saline, alkaline, and saline-alkaline stresses. *BMC Plant Biol.* **2016**, *16*, 124. [CrossRef]

56. Cao, C.; Long, R.; Zhang, T.; Kang, J.; Wang, Z.; Wang, P.; Sun, H.; Yu, J.; Yang, Q. Genome-Wide Identification of microRNAs in Response to Salt/Alkali Stress in Medicago truncatula through High-Throughput Sequencing. *Int. J. Mol. Sci.* **2018**, *19*. [CrossRef] [PubMed]

57. Arshad, M.; Gruber, M.Y.; Wall, K.; Hannoufa, A. An Insight into microRNA156 Role in Salinity Stress Responses of Alfalfa. *Front. Plant Sci.* **2017**, *8*. [CrossRef] [PubMed]

58. Wang, M.; Wang, Q.L.; Zhang, B.H. Response of miRNAs and their targets to salt and drought stresses in cotton (Gossypium hirsutum L.). *Gene* **2013**, *530*, 26–32. [CrossRef]

59. Si, J.-N.; Zhou, T.; Xu, F.; Bo, W.-H.; Wu, R.-L. Salt-responsive MicroRNAs in Populus euphratica by Deep Sequencing. *Bull. Botanical Res.* **2015**, *35*, 836–842.

60. Sathik, M.B.M. Identification and Validation of Cold Responsive MicroRNAs of Hevea brasiliensis Using High Throughput Sequencing. *J. Crop Sci. Biotechnol.* **2017**, *20*, 369–377.

61. Akdogan, G.; Tufekci, E.D.; Uranbey, S.; Unver, T. miRNA-based drought regulation in wheat. *Funct. Integr. Genom.* **2016**, *16*, 221–233. [CrossRef]

62. Tang, S.; Wang, Y.; Li, Z.; Gui, Y.; Xiao, B.; Xie, J.; Zhu, Q.-H.; Fan, L. Identification of wounding and topping responsive small RNAs in tobacco (Nicotiana tabacum). *BMC Plant Biol.* **2012**, *12*. [CrossRef]

63. Bukhari, S.A.H.; Shang, S.; Zhang, M.; Zheng, W.; Zhang, G.; Wang, T.-Z.; Shamsi, I.H.; Wu, F. Genome-wide identification of chromium stress-responsive micro RNAs and their target genes in tobacco (Nicotiana tabacum) roots. *Environ. Toxicol. Chem.* **2015**, *34*, 2573–2582. [CrossRef]

64. Long, R.-C.; Li, M.-N.; Kang, J.-M.; Zhang, T.-J.; Sun, Y.; Yang, Q.-C. Small RNA deep sequencing identifies novel and salt-stress-regulated microRNAs from roots of Medicago sativa and Medicago truncatula. *Physiologia Plantarum* **2015**, *154*, 13–27. [CrossRef] [PubMed]

65. Cai, C.; Guo, W.; Zhang, B. Genome-wide identification and characterization of SPL transcription factor family and their evolution and expression profiling analysis in cotton. *Sci. Rep.* **2018**, *8*. [CrossRef] [PubMed]

66. Yin, H.; Hong, G.; Li, L.; Zhang, X.; Kong, Y.; Sun, Z.; Li, J.; Chen, J.; He, Y. miR156/SPL9 Regulates Reactive Oxygen Species Accumulation and Immune Response in Arabidopsis thaliana. *Phytopathology* **2019**, PHYTO08180306R. [CrossRef]

67. Tao, Y.; Yuan, F.H.; Leister, R.T.; Ausubel, F.M.; Katagiri, F. Mutational analysis of the Arabidopsis nucleotide binding site-leucine-rich repeat resistance gene RPS2. *Plant Cell* **2000**, *12*, 2541–2554. [PubMed]

68. Zhu, Q.-H.; Fan, L.; Liu, Y.; Xu, H.; Llewellyn, D.; Wilson, I. miR482 Regulation of NBS-LRR Defense Genes during Fungal Pathogen Infection in Cotton. *PLoS ONE* **2013**, *8*. [CrossRef]

69. Suzuki, N.; Rivero, R.M.; Shulaev, V.; Blumwald, E.; Mittler, R. Abiotic and biotic stress combinations. *New Phytologist* **2014**, *203*, 32–43. [CrossRef] [PubMed]

70. Foyer, C.H.; Rasool, B.; Davey, J.W.; Hancock, R.D. Cross-tolerance to biotic and abiotic stresses in plants: A focus on resistance to aphid infestation. *J. Exp. Bot.* **2016**, *67*, 2025–2037. [CrossRef]

71. Chen, Q.; Li, M.; Zhang, Z.; Tie, W.; Chen, X.; Jin, L.; Zhai, N.; Zheng, Q.; Zhang, J.; Wang, R.; et al. Integrated mRNA and microRNA analysis identifies genes and small miRNA molecules associated with transcriptional and post-transcriptional-level responses to both drought stress and re-watering treatment in tobacco. *BMC Genom.* **2017**, *18*. [CrossRef]

72. Bolger, A.M.; Lohse, M.; Usadel, B. Trimmomatic: A flexible trimmer for Illumina sequence data. *Bioinformatics* **2014**, *30*, 2114–2120. [CrossRef]

73. Pertea, M.; Kim, D.; Pertea, G.M.; Leek, J.T.; Salzberg, S.L. Transcript-level expression analysis of RNA-seq experiments with HISAT, StringTie and Ballgown. *Nat. Protocols* **2016**, *11*, 1650–1667. [CrossRef]

74. Mortazavi, A.; Williams, B.A.; McCue, K.; Schaeffer, L.; Wold, B. Mapping and quantifying mammalian transcriptomes by RNA-Seq. *Nat. Methods* **2008**, *5*, 621–628. [CrossRef]

75. Young, M.D.; Wakefield, M.J.; Smyth, G.K.; Oshlack, A. Gene ontology analysis for RNA-seq: Accounting for selection bias. *Genome Biol.* **2010**, *11*. [CrossRef]

76. Mao, X.Z.; Cai, T.; Olyarchuk, J.G.; Wei, L.P. Automated genome annotation and pathway identification using the KEGG Orthology (KO) as a controlled vocabulary. *Bioinformatics* **2005**, *21*, 3787–3793. [CrossRef]

77. Wen, M.; Shen, Y.; Shi, S.; Tang, T. miREvo: An integrative microRNA evolutionary analysis platform for next-generation sequencing experiments. *BMC Bioinform.* **2012**, *13*. [CrossRef]

78. Friedlaender, M.R.; Mackowiak, S.D.; Li, N.; Chen, W.; Rajewsky, N. miRDeep2 accurately identifies known and hundreds of novel microRNA genes in seven animal clades. *Nucleic Acids Res.* **2012**, *40*, 37–52. [CrossRef]

79. Wu, H.-J.; Ma, Y.-K.; Chen, T.; Wang, M.; Wang, X.-J. PsRobot: A web-based plant small RNA meta-analysis toolbox. *Nucleic Acids Res.* **2012**, *40*, W22–W28. [CrossRef]

80. Zhou, L.; Chen, J.; Li, Z.; Li, X.; Hu, X.; Huang, Y.; Zhao, X.; Liang, C.; Wang, Y.; Sun, L.; et al. Integrated Profiling of MicroRNAs and mRNAs: MicroRNAs Located on Xq27.3 Associate with Clear Cell Renal Cell Carcinoma. *PLoS ONE* **2010**, *5*. [CrossRef] [PubMed]

81. Livak, K.J.; Schmittgen, T.D. Analysis of relative gene expression data using real-time quantitative PCR and the 2(T)(-Delta Delta C) method. *Methods* **2001**, *25*, 402–408. [CrossRef] [PubMed]